



High color rendering index in phosphorescent white organic light-emitting diodes using a yellowish-green dopant with broad light emission

Min Su Park, Hyun Jin Park, Oh Young Kim, Jun Yeob Lee*

Department of Polymer Science and Engineering, Dankook University, Jukjeon-dong, Suji-gu, Yongin-si, Gyeonggi-do 448-701, Republic of Korea

ARTICLE INFO

Article history:

Received 1 January 2013

Received in revised form 21 February 2013

Accepted 10 March 2013

Available online 29 March 2013

Keywords:

Color rendering index

White device

Yellowish green dopant

High efficiency

ABSTRACT

High color rendering index phosphorescent white organic light-emitting diodes (PHWOLEDs) were developed using a yellowish green dopant with broad light emission. A yellowish green phosphorescent dopant derived from difluorophenylquinoline ligand was synthesized and showed maximum emission peak at 550 nm and broad light emission with a full width at half maximum of 77 nm in addition to high quantum efficiency of 20.5%. The yellowish green dopant was used in PHWOLEDs to enhance the color rendering index and high color rendering index of 86.8 was obtained with a high quantum efficiency of 15.7%.

© 2013 Elsevier B.V. All rights reserved.

1. Introduction

Color rendering index (CRI) is one of important device performances of phosphorescent white organic light-emitting diodes (PHWOLEDs) for lighting applications. The CRI is a quantitative measure of the ability of a light source to reproduce the colors of various objects in comparison with a natural light source. Therefore, the CRI of PHWOLEDs can be improved by expanding the emission wavelength range of red, green and blue colors.

There have been many studies to increase the CRI of PHWOLEDs and most studies were devoted to balance red, green and blue emissions by developing new phosphorescent emitters and device architecture. It was first demonstrated that the CRI of PHWOLEDs can be improved by combining red, green and blue phosphorescent emitters in the emitting layer due to broadband emission of the emitter [1]. However, the CRI was rather limited because sky blue dopant material was used in the emitting layer [1]. Therefore, many studies were focused on developing

hybrid PHWOLEDs with deep blue fluorescent emitter and red/green phosphorescent emitters [2,3]. High CRI of 86 could be obtained by replacing the sky blue emitting phosphorescent dopant with a deep blue emitting fluorescent dopant [2]. High CRI above 90 was also reported using fluorescent emitters [4] and additional microlens film [5].

The use of deep blue phosphorescent emitter instead of sky blue phosphorescent emitter was also effective to achieve high CRI in PHWOLEDs [6–10]. Three color PHWOLEDs could achieve high CRI of up to 94 by utilizing a deep blue iridium dopant with a pyridylpyrazole type ligand and four emitting layer stack structure [10]. The other approach to increase the CRI of PHWOLEDs was to apply yellowish green dopant instead of common green dopant. Kwon et al. synthesized the yellowish green Ir complex with a peak emission wavelength of 535 nm and reported high CRI of 87 in three component PHWOLEDs due to compensation of weak emission in yellow emitting region [11]. Similar approach was also tried in the three color hybrid PHWOLEDs and high CRI of 91.2 was reported [12].

However, the yellowish green dopant materials reported in those works are not suitable for PHWOLEDs with a deep blue emitter with a peak emission at 460 nm and a

* Corresponding author. Tel./fax: +82 31 8005 3585.

E-mail address: leej17@dankook.ac.kr (J.Y. Lee).

deep red triplet emitter with a peak emission at 630 nm. In addition, the full width at half maximum (FWHM) was not broad enough to enhance the CRI of white devices. Therefore, a yellowish green dopant with a broad emission and a peak emission wavelength of around 550 nm is required.

In this work, we synthesized a novel yellowish-green iridium dopant with a peak emission wavelength of 550 nm and fabricated three complementary color PHWOLEDs using the yellowish-green dopant. A high quantum efficiency of 20.5% and a full width at half maximum of 77 nm were obtained in the yellowish-green device and a high quantum efficiency of 15.7% and high CRI of 86.8 were achieved in the PHWOLED fabricated using the yellowish-green dopant.

2. Experimental

Synthetic scheme of yellowish-green emitting iridium(III) bis(2-(2,4-difluorophenyl)quinoline) picolinate (FPQIrpic) compounds is described in Scheme 1.

2.1. Synthesis of 2-(2,4-difluorophenyl)quinoline

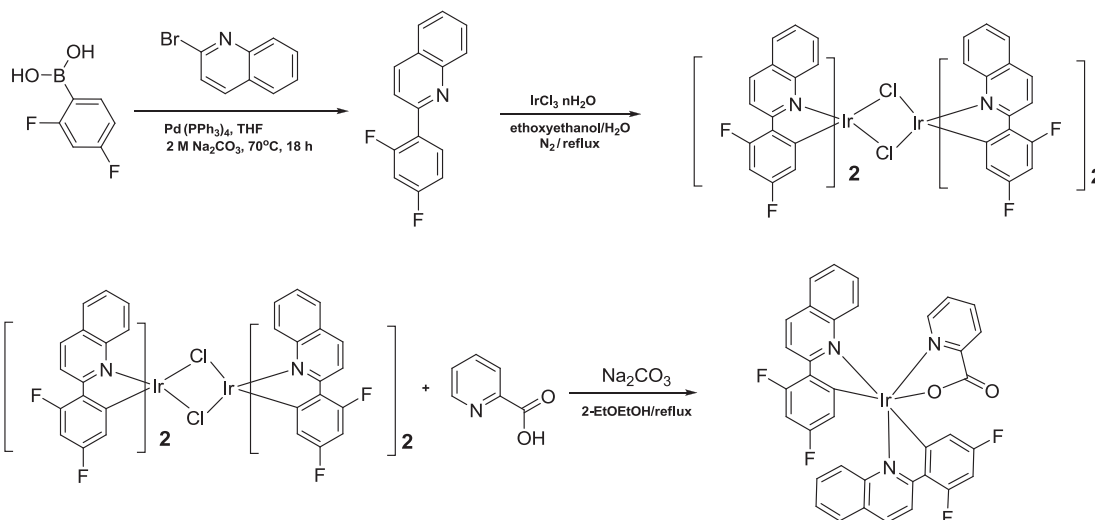
2-Bromoquinoline (5 g, 24.0 mmol), 2,4-difluorophenyl boronic acid (3.8 g, 24.0 mmol) and tetrakis(triphenylphosphine) palladium(0) ($\text{Pd}(\text{PPh}_3)_4$, 1.39 g, 1.20 mmol) were added to 2-neck flask and dissolved in tetrahydrofuran (50 ml). Aqueous sodium carbonate solution (2 M, 50 ml) was put into the solution and the solution was stirred at 70 °C for 18 h. The solution was cooled to room temperature and was poured into water followed by extraction with methylene chloride three times. The extract was dried over anhydrous magnesium sulfate and purified by column chromatography over silica using ethyl acetate: *n*-hexane (1:10) as an eluent to yield a pure white solid (5.1 g). Yield: 88%. $^1\text{H-NMR}$ (200 MHz, CDCl_3); 8.23–8.06 (m, 3H), 7.84 (d, $J = 8.0$ Hz, 2H), 7.74 (t, $J = 8.0$ Hz, 1H), 7.55 (t, $J = 8$ Hz, 1H), 7.10–6.90 (m, 2H).

2.2. Synthesis of iridium(III) bis(2-(2,4-difluorophenyl)quinoline) picolinate (FPQIrpic)

Iridium chloride hydrate (1.08 g, 3.62 mmol) and 2-(2,4-difluorophenyl)quinoline (2.5 g, 10.3 mmol) were dissolved in 2-ethoxyethanol:water (60 ml:20 ml) mixed solvent and the solution was refluxed for 22 h. The solution was cooled to room temperature and a yellow precipitate was filtered and washed with ethanol. The filtered precipitate was used for the subsequent reaction without further purification. The crude dimer was mixed with picolinic acid (1.53 g 12.43 mmol) and sodium carbonate (2.65 g, 25 mmol) in 2-ethoxyethanol (10 ml) and then refluxed for 18 h. The solution was cooled to room temperature and poured into water followed by extraction with methylene chloride. The organic layer was separated and solvent was subsequently evaporated. The residue was purified by column chromatography over silica using an ethyl acetate:*n*-hexane (1:20) as an eluent to yield 1.03 g of white powder (yield 36%) $^1\text{H-NMR}$ (500 MHz, dimethylsulfoxide (DMSO)); 8.67 (d, $J = 9.0$ Hz, 1H), 8.57–8.53 (m, 3H), 8.50 (d, $J = 8.7$ Hz, 1H), 8.075 (d, $J = 5.0$ Hz, 1H), 8.041 (d, $J = 8.0$ Hz, 1H), 7.99–7.97 (m, 1H), 8.65(t, $J = 3.0$ Hz, 1H), 7.62–7.54 (m, 4H), 7.46 (t, $J = 9.0$ Hz, 1H), 7.236 (d, $J = 9.0$ Hz, 1H), 7.088 (t, $J = 12.0$ Hz, 1H), 7.077 (t, $J = 1.5$ Hz, 1H) 6.891 (m, 1H), 6.276(d, $J = 9.5$ Hz, 1H), 5.702 (d, $J = 8.0$ Hz, 1H). $^{13}\text{CNMR}$ (125 MHz, DMSO); 97.8, 116.2, 119.5, 124.0, 125.3, 126.0, 126.5, 126.8, 128.0, 128.4, 128.6, 129.9, 131.0, 138.8, 140.0, 146.0, 146.9, 150.5, 153.3, 165.9, 169.8. MS (FAB) m/z 796 [(M + H) $^+$]. Anal. Calcd. For $\text{C}_{36}\text{H}_{20}\text{F}_4\text{IrN}_3\text{O}_2$: C, 54.40; H, 2.54; N, 5.29. Found: C, 54.43; H, 2.57; N, 5.25.

2.3. Device fabrication and measurements

The organic materials used in this work were N, N'-diphenyl-N,N'-bis-[4-(phenyl-m-tolyl-amino)-phenyl]-biphenyl-4,4'-diamine (DNTPD), N,N'-di(1-naphthyl)-N,



Scheme 1. Synthetic scheme of FPQIrpic.

N'-diphenylbenzidine (NPB), N,N'-dicarbazolyl-3,5-benzene (mCP), 1,3,5-tris(N-phenylbenzimidazol-2-yl) benzene (TPBI), diphenylphosphine oxide-4-(triphenylsilyl) phenyl (TSPO1), iridium(III) bis((3,5-difluoro-4-cyano-phenyl)pyridine) picolinate (FCNIrpic), bis-(1-phenylisoquinoline)(acetylacetonate)iridium(III) ($\text{Ir}(\text{pq})_2\text{acac}$), and FPQIrpic.

Device structure of yellowish-green device was ITO (50 nm)/DNTPD (60 nm)/NPB (5 nm)/mCP (25 nm)/TPBI:FPQIrpic (25 nm)/TSPO1 (20 nm)/LiF (1 nm)/Al (200 nm). Doping concentrations of FPQIrpic were 3%, 5% and 10%. White PHOLEDs were fabricated using the device structure of ITO (50 nm)/DNTPD (60 nm)/NPB (5 nm)/mCP (25 nm)/mCP:FCNIrpic (20 nm)/TPBI:FPQIrpic: $\text{Ir}(\text{pq})_2\text{acac}$ (5 nm)/TSPO1 (35 nm)/LiF (1 nm)/Al (200 nm). Doping concentrations of FCNIrpic were 10% and 20%, while the doping concentrations of FPQIrpic and $\text{Ir}(\text{pq})_2\text{acac}$ were 10% and 0.8%, respectively. Optimized white PHOLED had the $\text{Ir}(\text{pq})_2\text{acac}$ doping concentration of 0.5%. Device structures of the yellowish green and white PHOLEDs are shown in Fig. 1.

All devices were fabricated by vacuum thermal evaporation. Organic materials were deposited on ITO substrate cleaned by sonication in distilled water and isopropyl alcohol followed by ultraviolet/ O_3 treatment for 10 min. Deposition rate of organic materials were 0.1 nm/s except for dopant materials and vacuum pressure for thermal deposition was 2.0×10^{-6} torr. After organic film deposition, a cathode consisting of 1 nm LiF 200 nm of Al was deposited at a rate of 0.01 nm/s for LiF and 0.1–0.4 nm/s for Al. Devices were encapsulated with a glass lid after metal deposition. CaO getter was attached to the glass lid to capture moisture and oxygen.

The device performances of the PHOLEDs were measured with Keithley 2400 source measurement unit and CS1000 spectroradiometer. Lambertian distribution of light emission was assumed in all measurement of external quantum efficiency.

Ultraviolet–visible (UV–Vis) and photoluminescence (PL) spectra were obtained using UV–Vis spectrophotometer (Shimadzu, UV-2501PC) and fluorescence spectrophotometer (HITACHI, F-7000), respectively. Materials were dissolved in tetrahydrofuran at a concentration of 1.0×10^{-4} M for UV–Vis and PL measurements. ^1H nuclear

magnetic resonance (NMR) and ^{13}C NMR data were recorded using Varian 600 NMR spectrometer. Samples were dissolved in chloroform for ^1H and ^{13}C NMR measurement. The highest occupied molecular orbital (HOMO) of host materials was measured using cyclic voltammetry. Mass spectra of organic materials were recorded using mass spectrometer (JEOL, JMS-AX505AW) operated under fast atom bombardment (FAB) mode. Elemental analysis was carried out using Flash2000 (ThermoFisher).

3. Results and discussion

The yellowish-green dopant, FPQIrpic, was designed by modifying a common orange emitting $\text{Ir}(\text{pq})_2\text{acac}$ dopant material with a peak emission wavelength of 592 nm. As the emission wavelength of the yellowish-green dopant should be positioned around 550 nm, the FPQIrpic was designed to increase the bandgap of iridium bis(2-phenylquinoline)acetylacetonate ($\text{Ir}(\text{pq})_2\text{acac}$). It is well known that the highest occupied molecular orbital (HOMO) of $\text{Ir}(\text{pq})_2\text{acac}$ is localized on phenyl unit, while the lowest unoccupied molecular orbital (LUMO) is dispersed over quinoline unit [13]. Therefore, the substitution of electron withdrawing substituent such as F and CN on phenyl unit of phenylquinoline ligand can deepen the HOMO level and increase the bandgap of the dopant material. The bandgap of dopant material can be further increased by using a bulky picolinic acid instead of common acetylacetonate. Therefore, two F units were attached to the phenyl unit of phenylquinoline ligand and picolinic acid was used as an ancillary ligand to shift the emission to yellowish-green wavelength range.

The synthetic scheme of the heteroleptic FPQIrpic dopant is shown in Scheme 1. Main ligand of the FPQIrpic dopant, 2-(2,4-difluorophenyl)quinoline, was synthesized by Suzuki coupling reaction of 2-bromoquinoline with 2,4-difluorophenyl boronic acid prepared by lithiation and boration of 1,3-difluorobenzene using lithium di(isopropyl)amide. Synthetic yield of the ligand was 88%. The ligand was reacted with $\text{IrCl}_3 \cdot \text{nH}_2\text{O}$ and picolinic acid ancillary ligand to give FPQIrpic. The FPQIrpic dopant was purified by column chromatography to give high purity over 99% from high performance chromatography analysis.

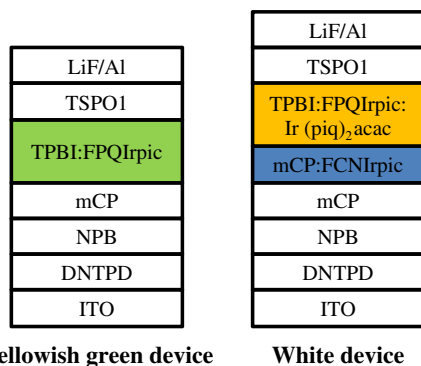


Fig. 1. Device structures of yellowish green and white PHOLEDs.

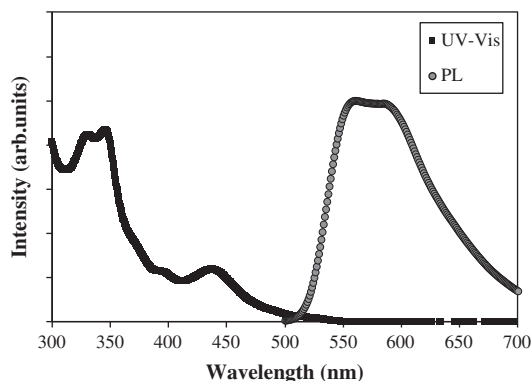


Fig. 2. UV–Vis and PL spectra of FPQIrpic.

Photophysical properties of FPQIrpic were analyzed using ultraviolet–visible (UV–Vis) and photoluminescence (PL) spectrometers. Fig. 2 shows UV–Vis and solution PL spectra of the FPQIrpic dopant. FPQIrpic exhibited strong absorption peaks below 345 nm which are assigned to $\pi-\pi^*$ absorption of FPQ ligand. Weak absorption was also observed above 438 nm, which is attributed to metal to ligand charge transfer absorption of FPQIrpic. The bandgap calculated from the absorption edge of the UV–Vis spectrum was 2.29 eV, which was wider than that of Ir(pq)₂acac (2.20 eV) without the F substituents. The two F substituents and bulky picolinic acid ancillary ligand induced the blue shift of the PL emission. Triplet emission of FPQIrpic was observed at 554 nm and it was shifted by 38 nm in comparison with 592 nm of Ir(pq)₂acac. The PL emission wavelength of the FPQIrpic dopant was in the yellowish green region. Full width at half maximum (FWHM) of FPQIrpic was 85 nm, which can be beneficial to obtain high CRI due to broad light emission over wide wavelength range.

The HOMO of FPQIrpic was measured by cyclic voltammetry using ferrocene as the standard material and the LUMO was calculated from the HOMO and the optical bandgap from UV–Vis measurement. The HOMO and LUMO of FPQIrpic were 5.51 eV and 3.22 eV, respectively. The HOMO of FPQIrpic was shifted by 0.31 eV compared to that of Ir(pq)₂acac due to electron withdrawing F substituents [14].

Yellowish-green devices of the FPQIrpic dopant were fabricated to evaluate the device performances of FPQIrpic. The device performances of the FPQIrpic device were optimized by changing the doping concentration of the FPQIrpic dopant. Fig. 3 shows current density–voltage curves of FPQIrpic devices according to doping concentration of FPQIrpic. The doping concentrations of FPQIrpic were 3, 5 and 10 wt%. There was little dependence of current density and luminance of FPQIrpic device on the doping concentration of FPQIrpic.

The quantum efficiency–luminance curves of FPQIrpic device are shown in Fig. 4. The quantum efficiency was also little affected by the doping concentration of FPQIrpic and similar quantum efficiency was obtained in the FPQIrpic device irrespective of doping concentration. However, the maximum quantum efficiency and quantum efficiency at 1000 cd/m² were 20.5% and 16.8%, respectively.

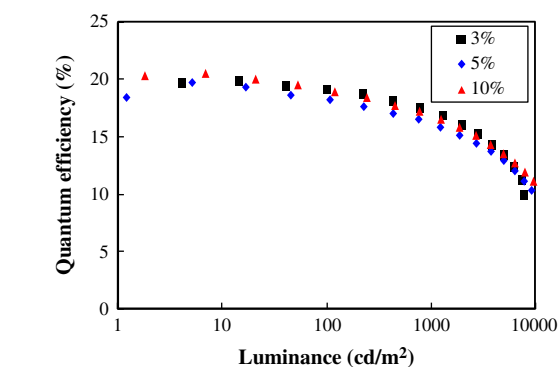


Fig. 4. Quantum efficiency–luminance curves of FPQIrpic devices according to doping concentration of FPQIrpic.

high luminance were high at 10% doping concentration. Therefore, 10% doping concentration was selected as the doping concentration for PHWOLEDs. The maximum quantum efficiency and quantum efficiency at 1000 cd/m² were 20.5% and 16.8%, respectively.

Electroluminescence (EL) spectra of the FPQIrpic PHOLEDs are represented in Fig. 5. The FPQIrpic PHOLEDs showed a maximum emission peak at 550 nm without any other emission peak irrespective of FPQIrpic doping concentration. This indicates the complete energy transfer from TPBI host to FPQIrpic dopant. The 550 nm emission of FPQIrpic was close to the middle of deep blue emission of FCNIrpic (458 nm) and deep red emission of Ir(piq)₂acac (630 nm). In addition, FWHM of FPQIrpic device was 77 nm, which is suitable for obtaining broad light emission. Compared with common tris(2-phenylpyridine) iridium with 55 nm FWHM in our measurement, the FWHM was increased by 22 nm. Therefore, the FPQIrpic dopant can be effective to increase the CRI of PHWOLEDs.

Based on the emission wavelength of FPQIrpic, three color PHWOLEDs were fabricated using deep blue emitting FCNIrpic, yellowish green emitting FPQIrpic, and deep red emitting Ir(piq)₂acac. Two emitting layers of mCP:FCNIrpic and TPBI:FPQIrpic:Ir(piq)₂acac were stacked to prepare the

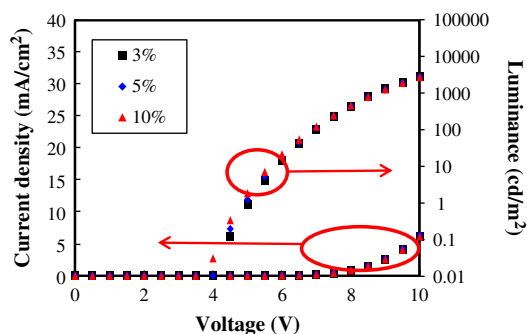


Fig. 3. Current density–voltage–luminance curves of FPQIrpic devices according to doping concentration of FPQIrpic.

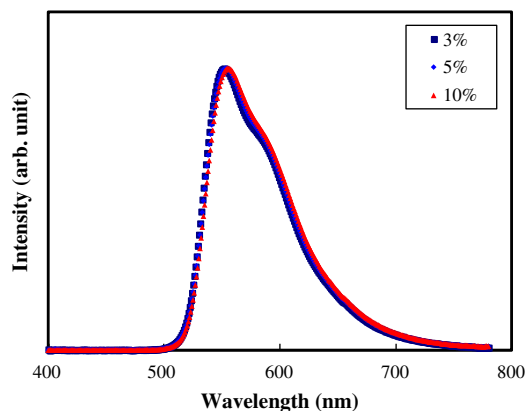


Fig. 5. Electroluminescence spectra of FPQIrpic devices according to doping concentration of FPQIrpic.

three color PHWOLEDs. Doping concentration of FCNIrpic was optimized to balance red, green and blue emissions. The doping concentration of FCNIrpic was changed from 10% to 20%, while the doping concentrations of FPQIrpic and $\text{Ir}(\text{piq})_2\text{acac}$ were fixed at 10% and 0.8%, respectively. Fig. 6 shows current density–voltage–luminance curves of PHWOLEDs according to the doping concentration of FCNIrpic. The current density and luminance of PHWOLEDs were increased according to the doping concentration of FCNIrpic and high current density and luminance were obtained at 20% doping concentration. The increase of current density at high doping concentration is due to better electron transport through FCNIrpic dopant materials.

Quantum efficiency–luminance curves of the PHWOLEDs are shown in Fig. 7. There was little difference of quantum efficiency according to the doping concentration of FCNIrpic and maximum quantum efficiency of the PHWOLEDs was 14.3–14.7%. The quantum efficiency at 1000 cd/m^2 was 11.3–11.5%. The similar quantum efficiency at different doping concentrations indicate that charge balance in the emitting layer is not affected by the doping concentration.

Electroluminescence (EL) spectra of the PHWOLEDs are presented in Fig. 8. Although there was little difference of quantum efficiency according to FCNIrpic doping concentration, the EL spectra of PHWOLEDs were greatly affected by the FCNIrpic doping concentration. All EL spectra were normalized to compare relative change of blue and red:–green emissions. The relative red:green intensity of the PHWOLEDs was decreased according to the increase of FCNIrpic doping concentration, indicating more blue emission at high FCNIrpic doping concentration. The high blue intensity at high doping concentration is related with the recombination zone shift caused by better electron transport properties at high FCNIrpic doping concentration [15]. In our study, it was found that electron transport properties of FCNIrpic doped emitting layer are improved at high doping concentration due to good electron transport properties of FCNIrpic, which shifted the recombination zone toward mCP:FCNIrpic, resulting in high blue intensity at high FCNIrpic doping concentration. The blue emission intensity was too strong at 20% doping concen-

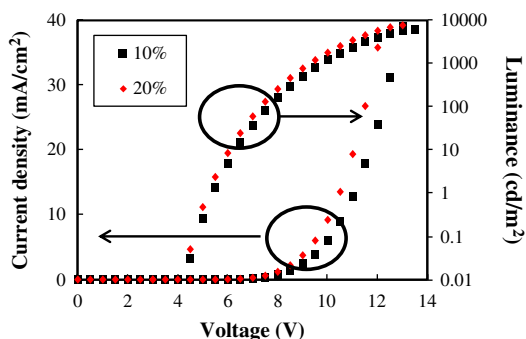


Fig. 6. Current density–voltage–luminance curves of white PHWOLEDs according to doping concentration of FCNIrpic. Device structure was ITO/DNTPD (60 nm)/NPB (5 nm)/mCP (25 nm)/mCP:FCNIrpic (20 nm)/TPBI:FPQIrpic:Ir(piq)₂acac (5 nm, 10%:0.8%)/TSPO1 (35 nm)/LiF (1 nm)/Al (200 nm).

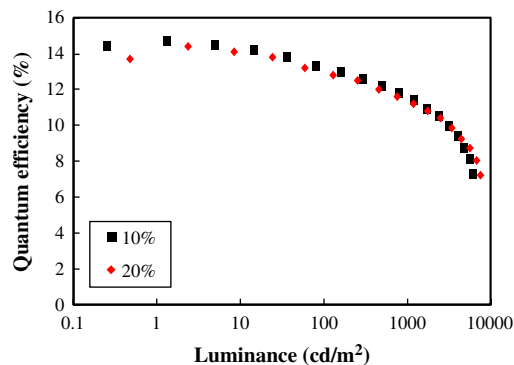


Fig. 7. Quantum efficiency–luminance curves of white PHWOLEDs according to doping concentration of FCNIrpic. Device structure was ITO/DNTPD (60 nm)/NPB (5 nm)/mCP (25 nm)/mCP:FCNIrpic (20 nm)/TPBI:FPQIrpic:Ir(piq)₂acac (5 nm, 10%:0.8%)/TSPO1 (35 nm)/LiF (1 nm)/Al (200 nm).

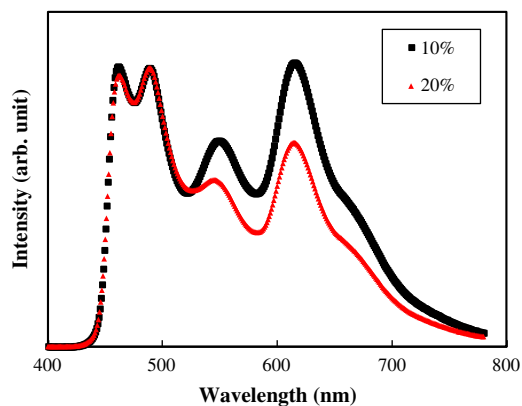


Fig. 8. Electroluminescence spectra of white PHWOLEDs according to doping concentration of FCNIrpic. Device structure was ITO/DNTPD (60 nm)/NPB (5 nm)/mCP (25 nm)/mCP:FCNIrpic (20 nm)/TPBI:FPQIrpic:Ir(piq)₂acac (5 nm, 10%:0.8%)/TSPO1 (35 nm)/LiF (1 nm)/Al (200 nm).

trations and it was balanced with red:green emission at 10% doping concentration. Therefore, the doping concentration of FCNIrpic was fixed at 10%. However, the green intensity was too weak at 0.8% red doping concentration due to energy transfer from green emitter to red emitter. Therefore, the doping concentration of red emitter was further optimized to obtain balanced red, green and blue emissions.

The doping concentration of FPQIrpic and FCNIrpic was fixed at 10% and the doping concentrations of $\text{Ir}(\text{piq})_2\text{acac}$ was changed from 0.8% to 0.5% to balance red, green and blue emissions. Fig. 9 shows EL spectra of PHWOLEDs with 0.5% $\text{Ir}(\text{piq})_2\text{acac}$ at different luminances. Green emission of the PHWOLEDs was intensified by changing the red doping concentration from 0.8% to 0.5% and balanced red, green and blue emissions were obtained. Additionally, the EL spectra were not greatly changed by the doping concentration. The color coordinates of the PHWOLEDs at 100 cd/m^2 , 1000 cd/m^2 and 3000 cd/m^2 were (0.36,0.38), (0.37,0.39) and (0.36,0.39), respectively. The color coordinate of the PHWOLED was within the Planckian locus and the color temperature was between 4370 K and

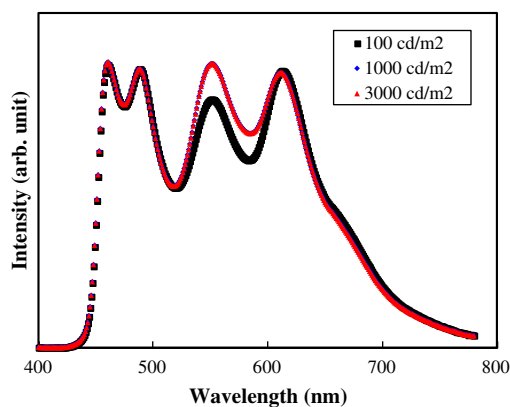


Fig. 9. Electroluminescence spectra of white PHOLEDs according to the luminance. Device structure was ITO/DNTPD (60 nm)/NPB (5 nm)/mCP (25 nm)/mCP:FCNlirpic (20 nm, 10%)/TPBI:FPQlirpic:Ir(piq)₂acac (5 nm, 10%:0.5%)/TSPO1 (35 nm)/LiF (1 nm)/Al (200 nm).

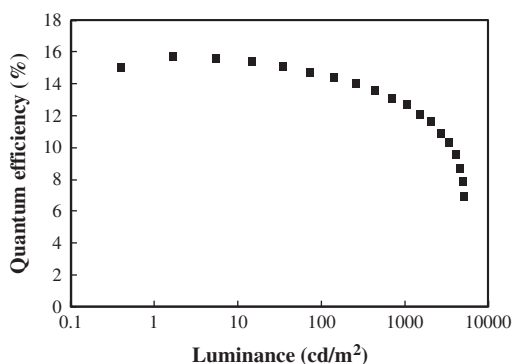


Fig. 10. Quantum efficiency–luminance curve of white PHOLED. Device structure was ITO (50 nm)/DNTPD (60 nm)/NPB (5 nm)/mCP (25 nm)/mCP:FCNlirpic (20 nm, 10%)/TPBI:FPQlirpic:Ir(piq)₂acac (5 nm, 10%:0.5%)/TSPO1 (35 nm)/LiF (1 nm)/Al (200 nm).

4700 K. The evenly distributed red, green and blue emissions improved the CRI of PHWOLEDs and the CRI values of the PHWOLEDs were 86.8, 86.4, and 85.0 at 100 cd/m², 1000 cd/m² and 3000 cd/m², respectively. High CRI value was achieved in the PHWOLEDs due to broad yellowish green emission of FPQlirpic. The emission peak at 550 nm which is in the middle of deep blue emitting FCNlirpic and deep red emitting Ir(piq)₂acac, and high FWHM of 77 nm increased the CRI of PHWOLEDs.

Quantum efficiency–luminance curve of the PHWOLED is shown in Fig. 10. Maximum quantum efficiency of 15.7% was obtained and the quantum efficiency at 1000 cd/m² was 12.7%. Although the quantum efficiency was not higher than the state of the art efficiency value of PHWOLEDs, it was better than that of other high CRI PHWOLEDs. The use of the high efficiency FPQlirpic yellowish-green dopant resulted in the high quantum efficiency.

4. Conclusions

In conclusion, a high efficiency dopant, FPQlirpic, was synthesized as a yellowish-green emitting material for PHWOLEDs and high CRI PHWOLEDs were effectively developed by using the yellowish-green dopant. The FPQlirpic dopant showed a maximum quantum efficiency of 20.5%, maximum emission peak of 550 nm and FWHM of 77 nm. High CRI of 86.8 was obtained in the three color PHWOLED doped with FCNlirpic, FPQlirpic and Ir(piq)₂acac because of balanced red, green and blue emissions. In addition, high quantum efficiency of 15.7% was achieved in the three color PHWOLEDs.

References

- [1] B.W. D'Andrade, M.E. Thompson, S.R. Forrest, *Adv. Mater.* 14 (2002) 147–151.
- [2] Y. Sun, N.C. Giebink, H. Kanno, B. Ma, M.E. Thompson, S.R. Forrest, *Nature* 440 (2006) 908–912.
- [3] G. Schwartz, M. Pfeiffer, S. Reineke, K. Walzer, K. Leo, *Adv. Mater.* 19 (2007) 3672.
- [4] G. Zhou, Q. Wang, C. Ho, W. Wong, D. Ma, L. Wang, *Chem. Commun.* (2009) 3574.
- [5] M. Thomschke, S. Reineke, B. Lussem, K. Leo, *Nano Lett.* 12 (2012) 424.
- [6] C.H. Chang, Y.J. Lu, C.C. Liu, Y.H. Yeh, C.C. Wu, *J. Disper. Technol.* 3 (2007) 193.
- [7] C.H. Yang, Y.M. Cheng, Y. Chi, C.J. Hsu, F.C. Fang, K.T. Wong, P.T. Chou, C.H. Chang, M.H. Tsai, C.C. Wu, *Angew. Chem. Int. Ed.* 46 (2007) 2418.
- [8] C.F. Chang, Y.M. Cheng, Y. Chi, Y.C. Chiu, C.C. Lin, G.H. Lee, P.T. Chou, C.C. Chen, C.H. Chang, C.C. Wu, *Angew. Chem. Int. Ed.* 47 (2008) 4542.
- [9] Y.C. Chiu, J.Y. Hung, Y. Chi, C.C. Chen, C.H. Chang, C.C. Wu, Y.M. Cheng, Y.C. Yu, G.H. Lee, P.T. Chou, *Adv. Mater.* 21 (2009) 2221.
- [10] C. Chang, K. Tien, C. Chen, M. Lin, H. Cheng, S. Liu, C. Wua, J. Hung, Y. Chiu, Y. Chi, *Org. Electron.* 11 (2010) 412.
- [11] D.M. Kang, J.-W. Kang, J.W. Park, S.O. Jung, S.-H. Lee, H.-D. Park, Y.-H. Kim, S.C. Shin, J.-J. Kim, S.-K. Kwon, *Adv. Mater.* 20 (2008) 2003.
- [12] S. Chen, G. Tan, W. Wong, H. Kwok, *Adv. Funct. Mater.* 21 (2011) 3785.
- [13] S. Lamansky, P. Djurovich, D. Murphy, F. Abdel-Razzaq, R. Kwong, I. Tsyba, M. Bortz, B. Mui, R. Bau, M.E. Thompson, *Inorg. Chem* 40 (2001) 1711.
- [14] S.H. Kim, J. Jang, J.Y. Lee, *Appl. Phys. Lett.* 91 (2007) 123509.
- [15] O.Y. Kim, H.J. Park, J.Y. Lee, *Appl. Phys. Lett.* submitted for publication (2013).